Old Dominion University
ODU Digital Commons

CCPO Publications   Center for Coastal Physical Oceanography

2002

Testing Ocean Tide Models in the Nordic Seas with Tidal Gravity Observations

M. S. Bos

T. F. Baker

K. Rothing

H.-P. Plag

Follow this and additional works at: https://digitalcommons.odu.edu/ccpo_pubs

Testing ocean tide models in the Nordic seas with tidal gravity observations

M. S. Bos,[1,*] T. F. Baker,[1] K. Røthing[2] and H.-P. Plag[2]

[1]*Proudman Oceanographic Laboratory, Bidston Observatory, Birkenhead,* CH43 7RA, *UK. E-mail: M.S.Bos@citg.tudelft.nl*
[2]*Norwegian Mapping Authority, Geodetic Institute, Kartverksveien* 21, N-3511 *Hønefoss, Norway*

SUMMARY

Tidal gravity observations at Ny-Ålesund on Spitzbergen, made with a LaCoste & Romberg gravimeter with electrostatic feedback, have been used to assess the accuracy of ocean tide models in the Nordic seas. Eight ocean tide models have been used to compute the ocean tide loading at Ny-Ålesund. The station is very close to the coast and therefore experiences a significant direct gravitational attraction of the nearby tidal water mass. For the bay adjacent to the station, the model values have been replaced by the tide gauge values and a special effort has been made to fit the models correctly to the coastline. The ocean tide models for M_2 and O_1 have also been compared with observations made over 30 years ago at Longyearbyen, Spitzbergen, with Askania gravimeters. The comparisons of the tidal gravity observations with computed ocean tide loading show that for the harmonic M_2 the phase lag of the ocean tide model of Schwiderski and the local tide model of Gjevik *et al.* are wrong by $+15°$ and $-5°$ in the Norwegian Basin. For the harmonic S_2, the models FES94.1, GOT00.2 and Schwiderski give a poor fit to the observed tidal loading at Ny-Ålesund because of phase lags that are too large in the Norwegian Basin by $\sim 10°$. FES94.1 and GOT00.2 also have S_2 amplitudes that are ~ 5 cm too large in the Norwegian Basin. For N_2, FES94.1, FES95.2, GOT00.2 and Schwiderski have phase lags that are $\sim 10°$ too large in the Norwegian Basin and FES94.1 and 95.2 also have N_2 amplitudes that are 2–4 cm too large in that region. Overall, for these three harmonics the global model FES99 gives the best fit to the tidal gravity observations at Ny-Ålesund and this agreement is even closer than that obtained using regional Arctic Ocean tide models.

Key words: gravity, Nordic Seas, tides.

1 INTRODUCTION

Satellite altimetry is an efficient tool for mapping the ocean tides. The satellite used most for this purpose is TOPEX/POSEIDON (TP) and this mission has produced many new global ocean tide models (Andersen *et al.* 1995; Shum *et al.* 1997). Unfortunately, the coverage of this satellite is restricted to the latitude range of $\pm 66°$. Other satellites with an altimeter radar such as GEOSAT and ERS1/2 have higher latitude limits of $72°$ and $82°$, respectively, but less accurate orbit determinations have limited their use in tidal studies (Smith 1999). Besides the lack of altimetry data in the polar regions, the number of tide gauges and bottom pressure recorders in this area is relatively small. Mostly, they are also of short observation length. Consequently, the hydrodynamic ocean tide models in the Arctic are only weakly constrained.

Using tidal gravity observations to test the ocean tide models in polar regions is therefore an interesting option. Whereas at mid-latitudes the gravity body tide of the Earth is typically a factor of 20 times the ocean tide loading, at higher latitudes the semi-diurnal and diurnal gravity body tide are much smaller (Baker 1984). This has the significant advantage that any error in the calibration of the tidal gravimeter has a much smaller effect relative to the ocean tide loading than is the case for mid-latitude tidal gravity stations. At the Poles the semi-diurnal and diurnal body-tide amplitudes are zero. Knopoff *et al.* (1989) and Agnew (1995) took advantage of this to use tidal gravity observations at the South Pole to test ocean tide models. Ny-Ålesund on Spitzbergen has a latitude of 78.9°N and at this latitude the M_2 gravity body tide is only 3.2 μgal (=32 nm s^{-2}). For the semi-diurnal harmonics the calibration error is smaller than the differences in the ocean tide loading values produced using different ocean tide models. However, at this latitude the O_1 gravity body tide still has an amplitude of over 13 μgal and so calibration errors are a limiting factor in the interpretation of the relatively small diurnal ocean tide loading.

In this research we use the tidal gravity observation made at Ny-Ålesund, Spitzbergen, with a LaCoste & Romberg gravimeter

with electrostatic feedback. Observations were also made at Longyearbyen, Spitzbergen, over 30 years ago (Melchior *et al.* 1970) using Askania gravimeters, as part of the Spitzbergen Astro-Geo-Project. We also compare these earlier observations with tidal loading models using recent M_2 and O_1 ocean tide models.

2 OCEAN TIDE MODELS

The Nordic seas are assumed to encompass the Norwegian Sea, Greenland Sea and the Barents Sea. Since these seas are located north of 66°, TP-based global ocean tide models such as CSR3.0, CSR4.0 (Eanes 1994) and GOT99.2b (Ray 1999) will not be discussed. Above this latitude these models become equal to FES94.1 (Le Provost *et al.* 1994). The new model of Ray (personal communication, 2001), GOT00.2, has assimilated both TP and ERS1/2 data and is for that reason included.

Other global ocean tide models used in this research are: Schwiderski (1980), abbreviated to SCHW, FES94.1, FES95.2 (Le Provost *et al.* 1988), FES99 (Lefèvre *et al.* 2002) and NAO.99b (Matsumoto *et al.* 2000). All of these models are barotropic and employ the Laplace tidal equations. Schwiderski uses an interpolation scheme to fit the model to tide gauge observations. NAO.99b is based on the same principles as SCHW but is given on a finer grid and is also constrained with TP data. FES94.1 is a pure hydrodynamic model, using a finite-element method to solve the tidal equations. FES95.2 is an update of FES94.1 with TP data assimilated into it and better Arctic ocean tides. The latest version of this series is FES99. The main improvement is the use, besides TP data, of a new set of 700 validated tide gauges in the assimilation process.

Two local tide models are also added to this list. One is the GNS ocean tide model (Gjevik & Straume 1989; Gjevik *et al.* 1994) and the other is by Kowalik & Proshutinsky (1993, 1994) called KP.

All models capture the main features of the tides. Only the Schwiderski model misses the amphidrome south of Spitzbergen for the semi-diurnal harmonics. This is probably caused by its coarse grid resolution of 1×1 deg^2. For the semi-diurnal harmonics, the tides in the Nordic seas are mainly driven by the tides in the North Atlantic Ocean that propagate into the Barents Sea and northwards into the Arctic Ocean. The Barents Sea is relatively shallow and large tidal amplitudes are found near the coast of Norway and at the entrance of the White Sea. In Fig. 1 the cotidal map of the M_2 harmonic is drawn. Note the almost constant phase lag in the Norwegian Basin. This results in a coherent ocean tide loading contribution of this region to the gravity stations on Spitzbergen. The ocean tide amplitudes in the Barents Sea are larger, but since the phase lag changes there more rapidly, loading contributions cancel each other and the total load is smaller than for the Norwegian Basin. It must also be noted that NAO.99b and GNS have South of Spitzbergen, in the Storfjorden, an amplitude that is almost double of that of the other models. NAO.99b also has a relatively large amplitude east of Spitzbergen. For harmonics S_2 and N_2, the pattern of the ocean tides is essentially the same as for M_2, although with smaller amplitudes and offsets in the phase lag. The ocean tides are distinctively different for K_1 and O_1 and their ocean tide loading is very small (see Section 4).

Furthermore, the seasonally changing ice coverage in the Arctic influences the dynamics of the tides. Kowalik & Untersteiner (1978) and Lyard (1997) have investigated this phenomenon and concluded that this affects only the tides in the south of the Barents Sea and at the entrance of the White Sea. This is fortunate since the loading contribution of these areas to stations on Spitzbergen is small
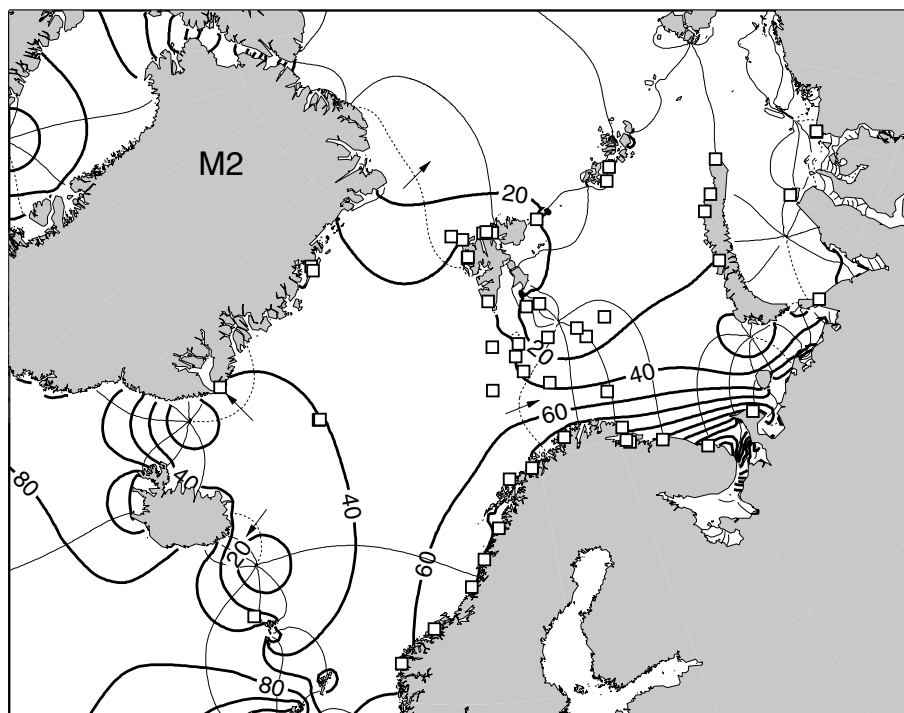
Figure 1. The ocean tides in the Nordic seas for harmonic M_2 as given by the FES99 model. The heavy lines represent the contours of equal amplitude with an interval of 20 cm. The thin contour lines indicate the phase lag with a contour interval of 45°. The phase lag is zero on the dotted line with the arrow indicating the direction of increasing phase lag. The white squares represent the location of the 52 tide gauges used in the comparison with the ocean tide models.

Table 1. The standard deviation between the tide gauges and ocean tide models. Units are in centimetres. The number of gauges used for each harmonic is given within parentheses.

Model	M_2 (52)	S_2 (42)	N_2 (38)	K_1 (50)	O_1 (39)
FES94.1	12.71	7.55	5.54	4.11	2.39
FES95.2	9.32	5.06	6.10	2.45	1.76
FES99	8.87	5.25	2.88	2.09	1.56
GNS	13.19	5.93	3.11	2.32	–
GOT00.2	8.81	7.51	4.13	3.25	2.36
KP	8.24	5.89	4.69	3.25	1.65
NAO.99b	9.02	5.66	4.21	3.02	1.79
SCHW	12.26	4.74	4.33	3.11	1.36

Table 2. The tide gauge observations at Ny-Ålesund and Longyearbyen, both given relative to the Greenwich meridian. The phase lags positive.

Harm.	Ny-Ålesund		Longyearbyen	
	(cm)	(deg)	(cm)	(deg)
M_2	45.65	3.9	52.2	356.0
S_2	16.91	49.6	19.9	40.0
N_2	8.99	338.4	10.0	329.6
K_1	6.40	247.9	6.9	220.0
O_1	2.21	90.1	3.1	76.1

(≈ 0.05 μgal for M_2). Changes in the tides caused by ice cover will therefore not influence the conclusions drawn in this research.

3 TIDE GAUGES

The simplest way to estimate the accuracy of the ocean tide models is by comparing them with tide gauges and bottom pressure recorders, although one must be aware that some of these gauges are assimilated into the models. Such a comparison has been performed by Lyard (1997) and has been repeated here with newer models. Table 1 contains the difference between the ocean tide models and 52 gauges of which the location is also given in Fig. 1. This difference is defined as the standard deviation σ between the gauge and model, averaged over one tidal cycle:

$$\sigma^2 = \frac{1}{2N} \sum_{i=1}^{N} \left| \mathbf{Z}_i^{\text{gauge}} - \mathbf{Z}_i^{\text{model}} \right|^2 . \tag{1}$$

Here $\mathbf{Z}^{\text{gauge}}$ and $\mathbf{Z}^{\text{model}}$ are the tides of the gauge and model given in their complex form. If one allows for small differences caused by the slightly different selection of gauges, these results are in good agreement with Lyard (1997).

Tide gauges with an observing period of less than 30 days are not used. The White Sea is also excluded from the comparison since the errors in this area are so large that they tend to dominate the comparison. The remaining 52 gauges were mostly obtained from the International Hydrographic Office and from Gjevik (personal communication, 1998).

In Table 1 one can see that FES94.1, GNS and SCHW have the largest errors with respect to the gauges for M_2. For FES94.1 this is mainly caused by large errors at the entrance of the White Sea. The errors of GNS and SCHW are more evenly distributed over the region. Note that GOT00.2, which is an adjustment of FES94.1, has for this harmonic a small standard deviation. Assimilating ERS1/2 data has thus improved the model. The ERS1/2 satellites have a Sun-synchronized orbit and this explains the lack of improvement for harmonic S_2. The differences with the tide gauges for GNS and SCHW are similar for S_2 to the other tide models. For harmonic N_2 the models FES94.1 and FES95.2 have the largest standard deviation with respect to the gauges. It will now be shown that the comparison of ocean tide loading with tidal gravity observations support these values and that this comparison can help to indicate where the errors are generated.

The ocean tide attraction on Spitzbergen produced by the tidal water in the bays in front of the stations forms a significant part of the total loading. To ensure accurate ocean tide loading values, the ocean tides in the bays are not taken from the ocean tide models but are assumed to be equal to the values measured at the tide gauges. These tide gauge values are given in Table 2.

4 OCEAN TIDE LOADING

For each harmonic the variation in gravitational acceleration at the surface of the Earth, **a**, owing to the weight of the ocean tides can be computed with (Farrell 1972)

$$\mathbf{a}(\mathbf{r}) = \int_A \rho \mathbf{Z}(\mathbf{r}') G(|\mathbf{r} - \mathbf{r}'|) \, dA. \tag{2}$$

The integral is taken globally over all tidal water masses and ρ is the average density of seawater. $\mathbf{Z}$ is again the complex tidal amplitude and G is a Green function that determines how much variation in gravity a point load of 1 kg at a distance of $|\mathbf{r} - \mathbf{r}'|$ causes at the station. The coordinates of the stations, together with the names of the gravimeters, are given in Table 3. The height above sea level is very important because the stations are so close to the coast. The distance of Ny-Ålesund to the water is 0.6 km, while for Longyearbyen this is 2.5 km.

The gravity Green function is written as the sum of an elastic and a Newtonian part. The elastic part describes the change in gravity caused by the vertical displacement of the station through the gravity field of the Earth. This produces gravity variations because the gravity field of the Earth decreases with height. In addition, the gravity field of the Earth will change because this deformation causes a redistribution of mass within the Earth.

The Newtonian part is caused by the vertical component of the direct gravitational attraction of the tidal water mass on the gravimeter. For stations exactly at sea level this is approximately 19 times smaller than the elastic part for small distances but for elevated sites it will become much larger. In Fig. 2 the Newtonian Green function is plotted for the two different heights of the stations. One can see that at the coast nearest to the stations, the Newtonian part exceeds the elastic part by one to two orders of magnitude. It is thus of the utmost importance to model the coastline correctly to obtain the correct amount of water attracting the gravimeter to obtain an accurate value for the ocean tide loading.

If the gravimeter is far away from the coast this problem can be avoided. Unfortunately, in the Arctic region the coast is mostly the only location available. Stations in the Antarctic suffer from the same problem (Sato *et al.* 1997) with the exception of the Amundsen–Scott station at the South Pole itself (Agnew 1995). To solve this problem, the high-resolution coastline provided by the plotting package GMT of Wessel & Smith (1996) has been used in the ocean

Table 3. The location of the gravimeters.

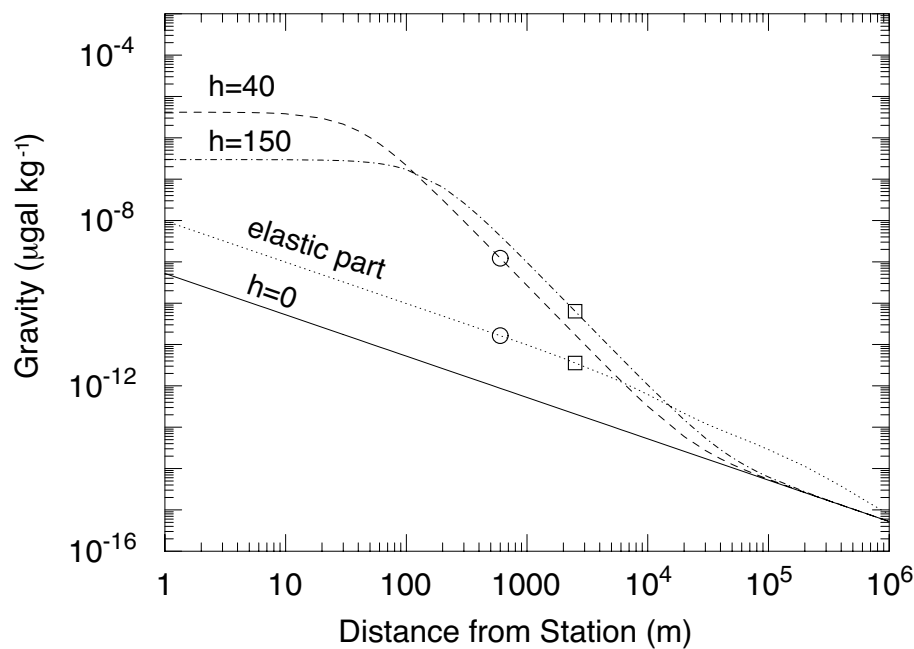| Place	Instr.	lat. (deg)	lon. (deg)	h (m)
Ny-Ålesund	LCR G-836F	78.9159	11.9385	40
Longyearbyen	Ask85a & 116	78.20	15.57	150

Figure 2. The Newtonian part of the Green function for the two heights of the stations. Also plotted is the elastic part of the Green function. The circles and squares represent the values on the coast nearest to Ny-Ålesund and Longyearbyen.
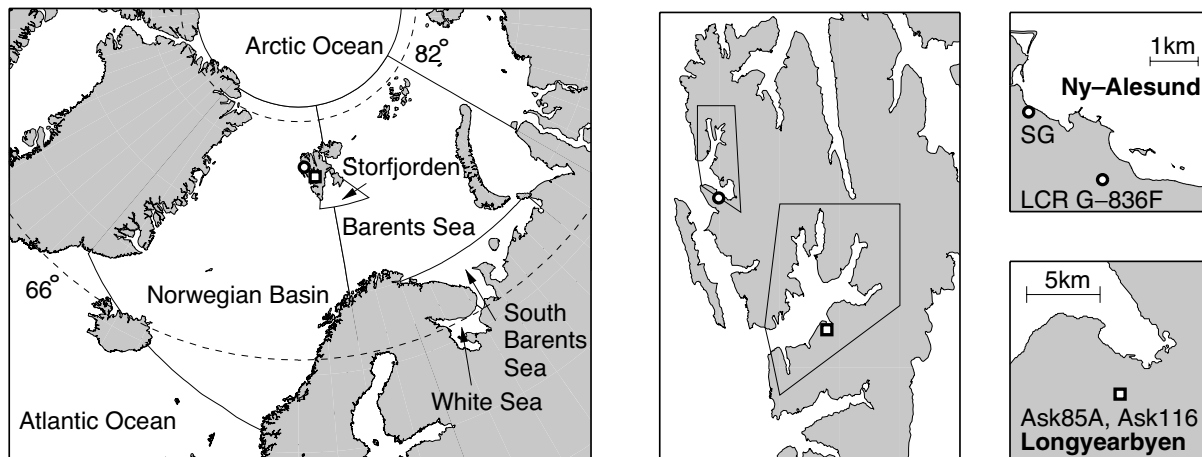

Figure 3. The location of the gravimeters at Ny-Ålesund and Longyearbyen and the definition of the regions in which the seas are divided. The dotted lines indicate the 66° northern latitude limit of the TOPEX/POSEIDON and 82° limit of the ERS1/2 satellites. The last two small figures on the right show the coastline near the stations in detail. At Ny-Ålesund also the location of the superconducting gravimeter (SG) of Sato *et al.* (2001) is drawn.

loading computation. At Ny-Ålesund this coastline data set was supplemented with a local map.

The importance of the nearby tidal water mass has been emphasized because Jentzsch *et al.* (2000) conclude that in the Arctic region, global ocean tide models can only explain 50 per cent of the observed loading. This is in disagreement with the findings in this research. A possible explanation is that they have not accurately modelled the attraction of the local tidal water mass. Another problem is the discretization of the ocean tide model. Most models are given on a 0.5×0.5 deg^2 grid, which is too coarse near the gravity stations to replace the integral in eq. (2) directly by a summation over the ocean grid cells. The models are therefore regridded, using simple bilinear interpolation, to a gradually finer grid. At Ny-Ålesund the smallest size of the gridboxes is $\sim$10 m. At the same time this regridding improves the fit of the ocean tide model with the coastline.

Since the aim of this research is the study of the ocean tide models in the Nordic seas, they are divided into regions as given in Fig. 3. The middle map in this figure shows the boundaries of the local bays. For each region the ocean tide loading has been calculated and for M_2 their values at Ny-Ålesund are given in Table 4. Here, and in all following tables, the gravity is defined with positive upwards and the phase is local and lags are negative.

In Table 4 one can see that the ocean loading contribution of NAO.99b in the Barents Sea has a phase that is $\sim$20°–30° retarded with respect to the other models. This is caused by a larger phase lag of NAO.99b between Nova Zembla and Spitzbergen. In this area the phase lag is not varying much and produces a coherent loading for stations on Spitzbergen. As a result NAO.99b has a relatively low total loading amplitude. NAO.99b also has high loading values for Storfjorden. This property is shared with GNS and is caused by the

Table 4. Contribution to the gravity ocean loading per region at Ny-Ålesund for harmonic M_2.

Model	Local bays		Oceans		Barents S.		Norwegian B.		Storfjorden		Sum	
	(µgal)	(deg)	(µgal)	(deg)	(µgal)	(deg)	(µgal)	(deg)	(µgal)	(deg)	(µgal)	(deg)
FES94.1	0.49	153.0	0.54	0.1	0.38	54.6	2.89	165.7	0.08	−143.2	2.81	154.7
FES95.2			0.56	−2.5	0.39	43.3	2.78	161.1	0.09	−150.2	2.65	150.1
FES99			0.55	2.0	0.42	51.1	2.98	164.5	0.08	−162.1	2.90	152.4
GNS	⋮	⋮	0.53	4.0	0.37	36.8	3.17	170.0	0.18	−145.4	3.02	162.2
GOT00.2			0.52	−3.9	0.47	44.9	2.89	165.4	0.06	−140.9	2.71	153.7
KP			0.54	6.4	0.52	44.1	3.09	162.9	0.09	−124.1	2.92	149.5
NAO.99b			0.57	4.0	0.40	20.9	2.84	163.0	0.16	−143.9	2.59	153.9
SCHW	0.49	153.0	0.52	0.1	0.48	51.9	2.78	149.5	0.10	131.3	2.93	135.0

fact that their tidal amplitudes are around 60 cm, while FES99 only has amplitudes of around 30 cm. Comparison with tide gauge has confirmed that GNS and NAO.99b are in error and not FES99. In this region SCHW has a distinctively different phase-lag for the loading, which is a consequence of its failure to model the amphidrome in this area.

Table 4 shows that the Norwegian Basin produces the largest ocean loading values at Ny-Ålesund. The ocean tide phase of SCHW in this basin is ∼15° smaller than for FES99 and KP, which is thus clearly reflected in the ocean loading values. For analogous reasons the phase of the loading of GNS in this basin is ∼5° larger.

The total ocean loading contribution of all areas except the local bays, Norwegian Basin, Barents Sea and Storfjorden is given under the name Oceans. The local tide models GNS and KP have been augmented with data from FES99 to make them global. For M_2 the ocean loading contributions of the Ocean region are all very similar. This is a good indication that this loading is well determined and that the differences in the total ocean tide loading values are mostly generated in the Nordic seas.

For S_2 and N_2 the relative importance of each region to the total ocean loading on Spitzbergen is the same as for M_2. The only difference is an overall reduced size of the amplitudes and an offset in the phase lags.

For harmonic O_1 the same breakdown per region of the ocean loading at Ny-Ålesund is given in Table 5. It shows that the contri-butions of the loading outside the Nordic seas are relatively more important and show larger differences. This makes assessing the accuracy of the ocean tide models in the Nordic seas much more difficult. The models FES99 and SCHW also show the problem of non-uniqueness of the ocean loading convolution integral. These two models have different values for the loading outside the Nordic seas and for the Norwegian Basin. Coincidentally, these two differences cancel each other, resulting in almost equal total ocean loading values. Owing to problems in observation of the gravity loading for diurnal harmonics (see Section 5), the diurnal ocean loading values will not be discussed further. The total ocean loading values at Ny-Ålesund for the other harmonics are given in Table 6. Longyearbyen is close enough to Ny-Ålesund to have the same properties for its ocean tide loading with only a larger influence of the Storfjorden. Its total ocean loading values for M_2 and O_1 are also listed in Table 6.

Recently, Sato *et al.* (2001) have computed the ocean tide loading for the superconducting gravimeter (SG) at Ny-Ålesund. The location of this instrument is shown in Fig. 3, and is approximately 100 m from the coast at a height of 44 m. The effect of the direct attraction of the tidal water mass in the bay on the gravimeter is even larger. For M_2 at the LCR G836-F spring gravimeter the effect of the bay is ∼0.4 µgal. At the SG this is 1.9 µgal, which is almost half of the total effect. An even higher-resolution map of the coastline would be necessary to model the loading contribution of the bay at

Table 5. Contribution to the gravity ocean loading per region at Ny-Ålesund for harmonic O_1.

Model	Local bays		Oceans		Barents S.		Norwegian B.		Storfjorden		Sum	
	(µgal)	(deg)	(µgal)	(deg)	(µgal)	(deg)	(µgal)	(deg)	(µgal)	(deg)	(µgal)	(deg)
FES94.1	0.02	79.6	0.12	−136.9	0.00	−151.4	0.20	127.0	0.01	137.9	0.24	152.3
FES99	0 02	79.6	0.09	−163.1	0.03	145.0	0.25	114.8	0.01	129.7	0.33	131.5
SCHW	0.02	79.6	0.08	−135.5	0.03	128.9	0.29	122.9	0.01	120.8	0.34	133.0

Table 6. The total ocean tide loading.

Model	Ny-Ålesund								Longyearbyen			
	M_2		S_2		N_2		O_1		M_2		O_1	
	(µgal)	(deg)	(µgal)	(deg)	(µgal)	(deg)	(µgal)	(deg)	(µgal)	(deg)	(µgal)	(deg)
FES94.1	2.81	154.7	1.26	96.9	0.82	166.5	0.24	152.3	2.41	150.6	0.25	145.9
FES95.2	2.65	150.1	1.02	108.0	0.79	164.2	0.28	140.7	2.29	146.9	0.29	138.1
FES99	2.90	152.4	1.01	106.9	0.61	174.7	0.33	131.5	2.51	147.4	0.34	129.0
GNS	3.02	162.2	1.10	114.5	0.65	173.8	−	−	2.66	160.8	−	−
GOT00.2	2.71	153.7	1.26	99.5	0.59	162.6	0.28	133.7	2.28	148.7	0.29	129.0
KP	2.92	149.5	1.15	110.7	0.69	172.5	0.36	148.1	2.43	145.1	0.37	144.9
NAO.99b	2.59	153.9	0.88	115.3	0.40	178.5	0.37	141.3	2.26	154.3	0.38	136.6
SCHW	2.93	135.0	1.14	93.4	0.59	161.0	0.34	133.0	2.65	126.8	0.34	127.3

Table 7. The observed gravimetric factor and phase at Ny-Ålesund and Longyearbyen.

Instrument	$M_2 \, \delta_{obs}$ (deg)	$S_2 \, \delta_{obs}$ (deg)	$N_2 \, \delta_{obs}$ (deg)	$O_1 \, \delta_{obs}$ (deg)
LCR G-836F	0.5335 ± 0.0054	1.1253 ± 0.0120	0.2044 ± 0.0293	1.1325 ± 0.0018
	(60.68 ± 0.31)	(36.79 ± 0.69)	(39.66 ± 1.68)	(1.08 ± 0.10)
Ask85a	0.6500 ± 0.0232	–	–	1.1925 ± 0.0133
	(47.12 ± 1.33)			(0.40 ± 0.76)
Ask116	0.5602 ± 0.0317	–	–	1.1412 ± 0.0088
	(46.96 ± 1.82)			(0.31 ± 0.51)

this site accurately enough to study the tides in the Nordic seas. This information was not available and therefore this location will not be discussed further.

For all global ocean tide models the tidal water mass was conserved by subtracting a uniform tidal layer from the models. This has a large effect on SCHW of $\sim$0.3 μgal for M_2. The other models are affected by 0.06 μgal or less, which is small. The Green function was taken from Francis & Mazzega (1990), which is based on the Preliminary Reference Earth Model (Dziewonski & Anderson 1981). Using a Green function based on another elastic Earth model such as the Gutenberg–Bullen model (Farrell 1972) only changes the ocean loading values by a maximal value of 0.013 μgal, which is negligible.

5 TIDAL GRAVIMETRY OBSERVATIONS

As mentioned before, the smallness of the body tide for the diurnal and semi-diurnal harmonics is beneficial to reducing the calibration error. A well-calibrated Askania or LaCoste & Romberg gravimeter has a scale calibration accuracy of better than 1 per cent (Baker *et al.* 1989), but assume for the moment it is 1 per cent. At Longyearbyen the amplitude of the body tide for M_2 is close to 3.65 μgal and this leads to a calibration error of only 0.0365 μgal. This is smaller than the differences between the computed gravity ocean loading values using different ocean tide models. For O_1 the amplitude of the body tide at Ny-Ålesund is 13.53 μgal. Taking again a calibration accuracy of 1 per cent this gives now an error of 0.14 μgal. Looking at Table 6 one sees that this error is larger than the ocean loading differences.

From 1969 until 1970, the Astro-Geo-Project Spitzbergen observed, among other things, tidal gravity variations at Longyearbyen. The actual measurements were taken by Bonatz & Melchior (1971) in a disused mine, 350 m under the surface. He used three Askania gravimeters and obtained for two of them, Ask85a and Ask116, a

data set of approximately 250 d each. The observation period for the third instrument was only 38 d and will be discarded because of the large uncertainties in the observations. The hourly values have been re-analysed with the ETERNA programme of Wenzel (1996) and are given in Table 7. Note that some observed gravimetric factors differ significantly from the gravimetric factors for the body tide. This is caused by the smallness of the body tide, which makes the ocean tide loading relatively large. These values are, within the formal errors, in agreement with Melchior *et al.* (1970) and Moens (1976).

In 1996, gravity measurements were started again in Spitzbergen but this time in Ny-Ålesund with a LaCoste & Romberg spring gravimeter of the Norwegian Mapping Agency. This instrument, LCR G836-F, has an electrostatic feedback system. The data set is 306 d long and local air pressure data were taken into account during the analysis. The instrument was last calibrated in 1992 on the calibration line in Hanover. The values of the observations at Longyearbyen and Ny-Ålesund are also listed in Table 7.

6 COMPARISON OF OCEAN TIDE LOADING WITH OBSERVATIONS

To compute the body tide use has been made of the tidal potential of Tamura (1987). The elastic gravimetric factors are taken from Dehant *et al.* (1999). They also list gravimetric factors for an inelastic non-hydrostatic Earth but this changes the body-tide amplitude by less than 0.007 μgal for the semi-diurnals. This indicates that the body tide is well determined for the present work and can be assumed to be known perfectly.

The different ocean loading values are added to the body tide and the results are given in Figs 4–6 for harmonics M_2, S_2, N_2 and O_1. In these phasor plots the body-tide vector lies along the in-phase axis because the phase is defined relative to the local meridian. Next, the phasor plots include the observations with the circle, indicating the formal error of the analysis.
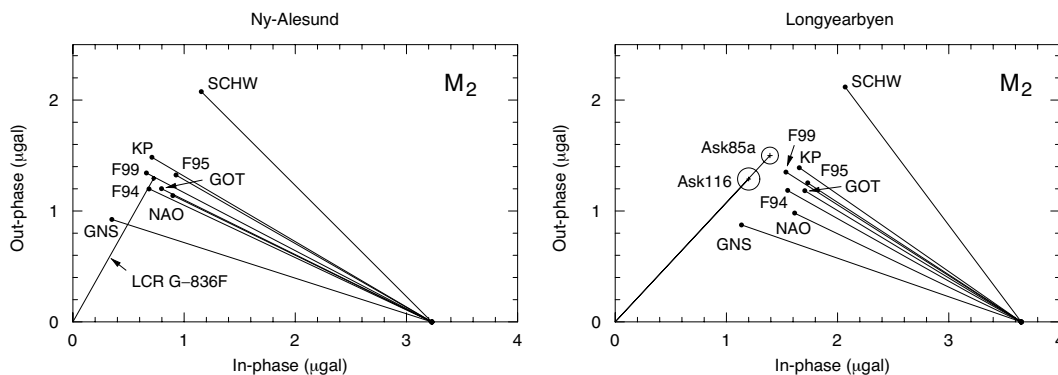

Figure 4. The ocean tide loading, body tide and observations for harmonic M_2 at Ny-Ålesund and Longyearbyen. The circles indicate the formal error of the analysis of the observations.
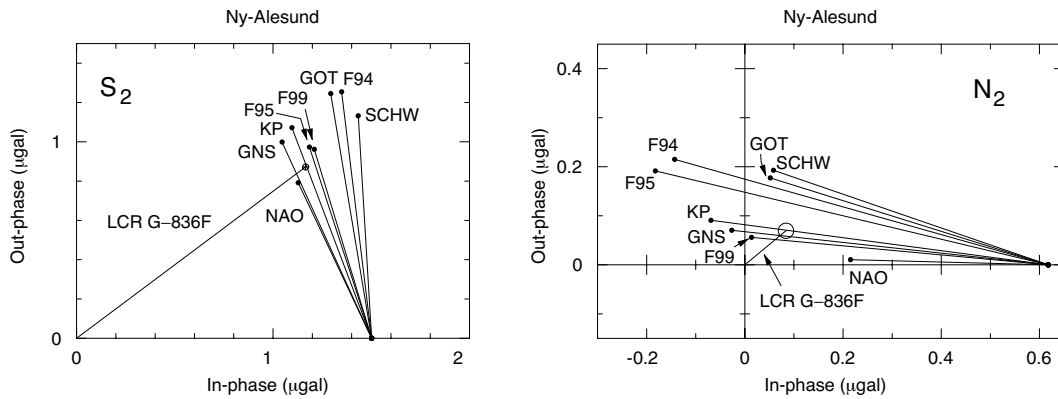
Figure 5. The ocean tide loading, body tide and observations for harmonic S_2 and N_2 at Ny-Ålesund.
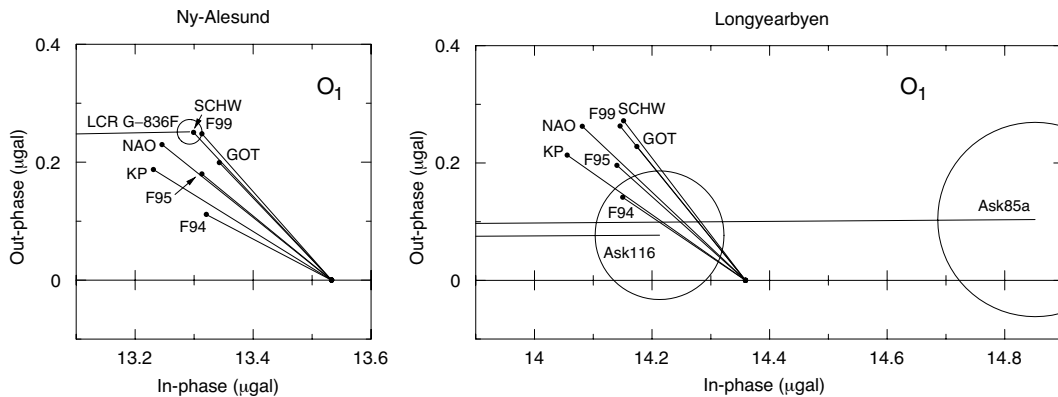

Figure 6. The ocean tide loading, body tide and observations for harmonic O_1 at Ny-Ålesund and Longyearbyen.

The Longyearbyen phasor plot for M_2 is similar to that of Moens (1976) who used an ocean tide map he compiled out of data found in the literature. For this harmonic he computed an ocean tide loading amplitude of 2.35 μgal and a phase of 142.5°, which is remarkably close to the values obtained with modern ocean tide models.

In Fig. 4 one sees that at Ny-Ålesund SCHW and GNS have distinct different loading values for M_2, which do not fit the observations. This is caused by the erroneous phase of −15° and +5° of these two models in the Norwegian Basin. The other differences are too small to clearly indicate a single source of misfit. At Longyearbyen the situation is similar but the amplitude of all loading values seem too small. Moens also encountered this problem. For M_2, FES99 is in closest agreement with the observations (approximately three times the formal rms error). An error in the published position or height of the Longyearbyen station could be a possible explanation, since this would affect the Newtonian attraction of the nearby tidal water masses.

The left-hand plot in Fig. 5 shows the same comparison for S_2. Now the GNS performs much better while SCHW, FES94.1 and GOT00.2 are the outliers. This is caused by their larger phase lag of ∼10° in the Norwegian Basin. Extra differences are caused in FES94.1 and GOT00.2 by larger amplitudes of 20–25 cm instead of 15–20 cm and extremely large amplitudes of 60 cm in the Storfjorden.

The results for N_2 are given in the right-hand plot of Fig. 5. This time the outliers are FES94.1 and FES95.2. Lyard (1997) did not compute his Arctic tides for N_2, which means that in the FES95.2 release it has remained very much the same as FES94.1. An extra phase lag of ∼10° in the Norwegian Basin is again the reason why

FES94.1, FES95.2, GOT00.2 and SCHW are different from the rest. The amplitudes of FES94.1 and FES95.2 are 2–4 cm larger than the average 9 cm in the middle of the basin. In GOT00.2 this amplitude has been reduced by the assimilation of ERS1/2 data.

For all three mentioned harmonics the ocean loading contribution of NAO.99b in the Barents Sea is ∼10°–30° larger than the rest. This does not influence the total loading value much for M_2 and S_2 and is partly compensated by the larger loading contribution of the Storfjorden. Perhaps future tidal gravity measurements on Nova Zembla could investigate the ocean tides in the Barents Sea in more detail. For N_2 the different phase lag of the loading contribution of this sea is noticeable and in addition the tidal amplitude of NAO.99b is 1 cm smaller in the Norwegian basin.

FES99 and KP fit the observations quite well at all three harmonics but none of them falls within the error of the observations at Ny-Ålesund. The misfit for FES99 is approximately 3 per cent of the total loading for M_2 and 11–12 per cent for S_2 and N_2. This means that, assuming the calibration is correct, that these observations can be used to test future ocean tide models in this area.

Finally, the results for harmonic O_1 are given in Fig. 6. Here the influence of any calibration error is significant. FES99 and SCHW give a good fit to the O_1 observations at Ny-Ålesund, which suggests that the calibration errors are small. At Longyearbyen the formal error of the observations is very large and the Askania gravimeter number 85a seems to suffer from a scale calibration error of around 4.5 per cent. Francis (personal communication, 2002) has commented that a few years ago, Melchior determined that this calibration factor was wrong by several per cent, which is consistent with the present work.

7 CONCLUSIONS

The hydrodynamic ocean tide models in the Nordic seas are only weakly constrained owing to the relatively small number of tide gauges and bottom pressure recorders in this area. The region also falls outside the range of the TP altimetry satellite, which is mostly used to map the ocean tides. It is therefore interesting to study the tides in the Nordic seas with tidal gravity observations that measure the ocean tides in the form of ocean tide loading. This study is greatly helped by the fact that the diurnal and semi-diurnal body tides are small at high latitudes. This reduces the calibration error for the semi-diurnal harmonics to below the differences between the ocean tide loading values. For the diurnal harmonics this error is still significant.

A conventional comparison of tide gauge data with the ocean tide models was also performed. For M_2 this comparison shows for most models a standard deviation of 8–9 cm. The models FES94.1, GNS and SCHW have a distinctively worse fit of 12–13 cm. The reason for their larger error is that FES94.1 has bad tidal values at the entrance of the White Sea and that the phase lags of SCHW and GNS are wrong by $+15°$ and $-5°$ in the Norwegian Basin. The last effect is clearly observed in the tidal gravity observations at Ny-Ålesund and confirmed with the observations at Longyearbyen. For S_2 the standard deviation of the models with the gauges is around 5–6 cm, while for FES94.1 and GOT00.2 this value is 7.5 cm. This is again caused by a wrong phase lag of the models in the Norwegian Basin by an amount of $\sim10°$ and a 5 cm larger amplitude in this area above the average of 15–20 cm. The gravity observations at Ny-Ålesund validate this conclusion. FES94.1 and FES95.2 suffer from the same problem for N_2. The amplitudes are now 2–4 cm larger than the average value of approximately 9 cm. In light of these results it would be better if TP-based global ocean models such as CSR4.0 replaced FES94.1 with another model to fill in the Nordic seas.

Overall, FES99 gives the closest fit for the above harmonics to the tidal gravity observations at Ny-Ålesund. The agreement is even closer than for the regional Arctic ocean tide models.

ACKNOWLEDGMENTS

REFERENCES

Agnew, D.C., 1995. Ocean-load tides at the South Pole: a validation of recent ocean-tide models, *Geophys. Res. Lett.,* **22,** 3063–3066.

Andersen, O.B., Woodworth, P.L. & Flather, R.A., 1995. Intercomparison of recent ocean tide models, *J. geophys. Res.,* **100,** 25 261–25 282.

Baker, T.F., 1984. Tidal deformations of the Earth, *Sci. Prog. Oxf.,* **69,** 197–233.

Baker, T.F., Edge, R.J. & Jeffries, G., 1989. European Tidal Gravity: an improved agreement between observations and models, *Geophys. Res. Lett.,* **16,** 1109–1112.

Bonatz, M. & Melchior, P., 1971. Erdgezeitenregistrierungen in der Arktis, *Obs. Roy. Belg. Comm. B, 58,* Sér. Géoph., **102,** 305–309.

Dehant, V., Defraigne, P. & Wahr, J.M., 1999. Tides for a convective Earth, *J. geophys. Res.,* **104,** 1035–1058.

Dziewonski, A.M. & Anderson, D.L., 1981. Preliminary reference earth model, *Phys. Earth planet. Inter.,* **25,** 297–356.

Eanes, R.J., 1994. Diurnal and semidiurnal tides from TOPEX/POSEIDON altimetry, *EOS, Trans. Am. geophys. Un.,* **75,** 108.

Farrell, W.E., 1972. Deformation of the Earth by surface loads, *Rev. Geophys. Space Phys.,* **10,** 761–797.

Francis, O. & Mazzega, P., 1990. Global charts of ocean tide loading effects, *J. geophys. Res.,* **95,** 11 411–11 424.

Gjevik, B. & Straume, T., 1989. Model simulations of the M2 and the K1 tide in the Nordic Seas and Arctic Ocean, *Tellus,* **41A,** 73–96.

Gjevik, B., Nøst, E. & Straume, T., 1994. Model simulations of the tides in the Barents Sea, *J. geophys. Res.,* **99,** 3337–3350.

Jentzsch, G., Knudsen, P. & Ramatschi, M., 2000. Ocean tidal loading affecting precise geodetic observations on Greenland: error account of surface deformations by tidal gravity measurements, *Phys. Chem. Earth,* **25,** 401–407.

Knopoff, L., Rydelek, P.A., Zürn, W. & Agnew, D.C., 1989. Observation of load tides at the South-Pole, *Phys. Earth planet. Inter.,* **54,** 33–37.

Kowalik, Z. & Proshutinsky, A.Y., 1993. Diurnal tides in the Arctic Ocean, *J. geophys. Res.,* **98,** 16 449–16 468.

Kowalik, Z. & Proshutinsky, A.Y., 1994. The Arctic ocean tides, in *The Polar Oceans,* eds Johannessen, O.M., Muench, R.D. & Overland, J.E., Vol. 85, Geophysical Monograph, American Geophysical Union.

Kowalik, Z. & Untersteiner, N.A., 1978. A study of the M2 tide in the Arctic Ocean, *Deutsche Hydr. Zeitsch.,* **32,** 216–229.

Le Provost, C., Lyard, F., Molines, J.M., Genco, M.L. & Rabilloud, F., 1988. A hydrodynamic ocean tide model improved by assimilating a satellite altimeter-derived data set, *J. geophys. Res.,* **103,** 5513–5529.

Le Provost, C., Genco, M.L., Lyard, F., Vincent, P. & Canceil, P., 1994. Spectroscopy of the world ocean tides from a finite-element hydrodynamic model, *J. geophys. Res.,* **99,** 24 777–24 797.

Lefèvre, F., Lyard, F.H., Le Provost, C. & Schrama, E.J.O., 2002. FES99: a tide finite element solution assimilating tide gauge and altimetric information, *J. Atmos. Oceanic Technol.,* **19,** in press.

Lyard, F.H., 1997. The tides in the Arctic Ocean from a finite element model, *J. geophys. Res.,* **102,** 15 611–15 638.

Matsumoto, K., Takanezawa, T. & Ooe, M., 2000. Ocean tide models developed by assimilating TOPEX/POSEIDON Altimeter data into hydrodynamical model: a global model and a regional model around Japan, *J. Oceanog.,* **56,** 567–581.

Melchior, P., Bonatz, M. & Blankenburgh, J., 1970. Astro-geo project Spitsbergen, *Obs. Roy. Belg. Comm. B, 52, Sér. Géoph.,* **98,** 1–15.

Moens, M., 1976. Solid Earth tide and Arctic Ocean loading tide at Longyearbyen (Spitsbergen), *Phys. Earth planet. Inter.,* **13,** 197–211.

Ray, R.D., 1999. A global ocean tide Model from TOPEX/POSEIDON Altimetry: GOT99.2, *NASA Technical Memorandum 209478.*

Sato, T., Ooe, M., Nawa, K., Shibuya, K., Tamura, Y. & Kaminuma, K., 1997. Long-period tides observed with a superconducting gravimeter at Syowa station, Antartica, and their implication to global ocean tide modeling, *Phys. Earth planet. Inter.,* **103,** 39–53.

Sato, T. *et al.*, 2001. Continuous gravity observation at Ny-Ålesund, Svalbard, Norway with a superconducting gravimeter CT#039, *J. geol. Soc. Japan,* **47,** 341–346.

Schwiderski, E.W., 1980. On charting global ocean tides, *Rev. Geophys. Space Phys.,* **18,** 243–268.

Shum, C.K. *et al.*, 1997. Accuracy assesment of recent ocean tide models, *J. geophys. Res.,* **102,** 25 173–25 194.

Smith, A.J.E., 1999. Application of satellite altimetry for global ocean tide modelling, *PhD thesis,* Delft University of Technology.

Tamura, Y., 1987. A harmonic development of the tide-generating potential, *Bulletin Inform. Marées Terres.,* **99,** 6813–6855.

Wenzel, H.G., 1996. The Nanogal Software: Earth tide data processing package ETERNA 3.30, *Bulletin d'Information Marées Terrestres,* **124,** 9425–9439.

Wessel, P. & Smith, W.H.F., 1996. A global, self-consistent, hierarchical, high-resolution shoreline database, *J. geophys. Res.,* **101,** 8741–8743.